

REMOVAL OF AN ACID DYE FROM AQUEOUS SOLUTIONS BY ADSORPTION ON A COMMERCIAL GRANULAR ACTIVATED CARBON: EQUILIBRIUM, KINETIC AND THERMODYNAMIC STUDY

Marius Sebastian Secula^{1*}, Benoît Cagnon², Igor Crețescu¹,
Mariana Diaconu¹, Stelian Petrescu¹

¹“Gheorghe Asachi” Technical University of Iași,

Faculty of Chemical Engineering and Environmental Protection,

73 Prof. Dr. Docent Dimitrie Mangeron Street, 700050 Iași, Romania

²ICOA – Institut de Chimie Organique et Analytique, CNRS-UMR 6005,
Institut Universitaire de Technologie, Université d'Orléans, 16 Rue d'Issoudun,
BP 16729, 45067 Orléans cedex 02, France

*Corresponding author: mariussecula@ch.tuiasi.ro

Received: August 10, 2011

Accepted: September 15, 2011

Abstract: The present paper approaches the study of the adsorption of an acid dye on a commercial granular activated carbon (GAC). Batch experiments were conducted to study the equilibrium isotherms and kinetics of Indigo Carmine on GAC. The kinetic data were analyzed using the Lagargren, Ho, Elovich, Weber-Morris and Bangham models in order to establish the most adequate model that describes this process, and to investigate the rate of IC adsorption. Equilibrium data were fitted to Langmuir and Freundlich isotherms. Langmuir isotherm equilibrium model and Ho kinetic model fitted best the experimental data.

The effects of temperature (25 – 45 °C), initial concentration of dye (7.5 – 150 mg·L⁻¹), GAC dose (0.02 – 1 g·L⁻¹), particle size (2 – 7 mm in diameter), solution pH (3 – 11) on GAC adsorption capacity were established. The adsorption process is found to be favored by a neutral pH, high values of temperature and small particle sizes. The highest adsorption capacity (133.8 mg·g⁻¹) of the GAC is obtained at 45 °C. The removal efficiency increases with GAC dose at relatively low initial concentrations of dye. Thermodynamic parameters such as standard enthalpy (ΔH), standard entropy (ΔS) and standard free energy (ΔG) were evaluated. The adsorption of Indigo Carmine onto GAC is an endothermic process.

Keywords: adsorption, equilibrium, granular activated carbon, Indigo Carmine, intraparticle diffusion, kinetics

INTRODUCTION

In recent years, the negative effect of dye wastewater on the ecological environment has brought about wide concern. At present, various methods and their combinations are used to treat dye wastewater; among them, it can be mentioned: biological treatment [1], ozonation [2], chemical coagulation [3], activated carbon adsorption [4] and electrocoagulation [5]. In a previous work we have described the removal of Indigo Carmine by electrocoagulation [6].

The adsorption technique has been proved to present an outstanding capability for efficiently removing a broad range of adsorbates [7]. Removal of dyes by adsorption has become of great importance due to their chemical and biological stability to conventional water treatment methods and the continuous growing need for high quality treatment. Activated carbon is one of the most widely used adsorbent materials due to its effectiveness and versatility.

Recently, electrochemical oxidation processes have attracted an increasing scientific and technical attention due to their high efficiency, ease operation and environmental compatibility [8]. Involving the use of GAC for adsorption and to increase the specific surface area of the electrode in order to oxidize the pollutant, the technology of three-dimensional electrode has been successfully applied to remove Acid Orange 7 dye from aqueous solutions [9].

Having in view the study of Indigo Carmine removal by means of a three-dimensional electrode reactor, the main purpose of this work is to study the simple adsorption process of Indigo Carmine onto a commercial GAC in order to determine the adsorption capacity of this adsorbent material, and to establish the kinetics and thermodynamic parameters for this adsorption system.

EXPERIMENTAL

Materials

The granular activated carbon (GAC) material was purchased from Romcarbon, Romania. This was washed several times with water to remove surface impurities, followed by drying at 120 °C for 24 h.

The porosity of GAC was determined through conventional nitrogen adsorption-desorption isotherm at -196 °C using a Micromeritics ASAP 2020. The samples were previously degassed at 250 °C for 48 h under a residual vacuum of less than 10⁻⁴ Pa. Thus, for the commercial GAC there were determined the following textural characteristics: specific microporous volume of 0.48 cm³·g⁻¹, total microporous volume of 0.66 cm³·g⁻¹, mean pore size of 1.62 nm, BET surface of 1403 m²·g⁻¹, external surface of 38 m²·g⁻¹, microporous surface of 631 m²·g⁻¹ and total surface of 631 m²·g⁻¹.

Indigo Carmine (Fig. 1), which is also commonly known as Acid Blue 74 or Food Blue 1 or FD & C Blue 2 (CASRN 860-22-0), is a dark blue, water-soluble powder. The molecular formula of the dye is C₁₆H₈O₈N₂S₂Na₂ and molecular weight is 466.36 g·mol⁻¹.

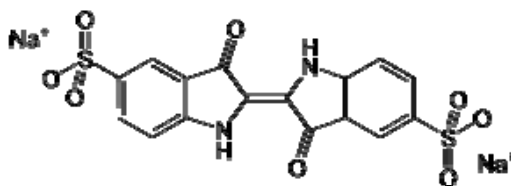


Figure 1. Molecular structure of Indigo Carmine

Stock solution of 1 g·L⁻¹ Indigo Carmine (Sigma Aldrich) was prepared by dissolving the dye in ultrapurified water. Having a resistivity higher than 18.2 MΩ·cm at 25 °C, the ultrapurified water was obtained by passing distilled water through a Barnstead Easypure II Thermo Scientific Water Purification System.

Adsorption studies

In the kinetic studies, 1 g of GAC was added to 1000 mL solution of Indigo Carmine. The initial concentrations of Indigo Carmine (C_0) ranged from 10 to 50 ppm. All kinetic experiments were performed at 175 rpm using a thermostated orbital shaker. At time = 0 and selected time intervals, 4 mL samples were extracted from the vessel using a 10 mL syringe.

The evolution of Indigo Carmine concentration during adsorption was followed by withdrawing 5 mL samples at predetermined time intervals. Samples were filtered by means of Wattman 0.45 μm filters. The concentration of Indigo Carmine was determined at $\lambda = 612$ nm using a Thermo Scientific Helios Epsilon UV/VIS spectrophotometer, which was previously calibrated. A Consort C863 multi-parameter analyzer, with a combined glass electrode was used for pH measurements.

In the equilibrium experiments for adsorption isotherms, 0.1 g of GAC was added to 100 mL solution of Indigo Carmine in 250 mL glass vessels. The initial concentration of dye was varied from 7.5 to 150 mg·L⁻¹. Equilibrium experiments were performed at three values of temperature: 25, 35 and 45 °C.

In order to establish the effect of GAC dose, pH value and particle size, several batch experiments were carried out.

The amount of Indigo Carmine adsorbed at equilibrium, q_e (mg·g⁻¹) was calculated by:

$$q_e = \frac{(C_0 - C_e)V}{W} \quad (1)$$

where C_0 and C_e (mg·L⁻¹) are the initial and equilibrium Indigo Carmine concentrations, respectively; V - the solution volume (L), W - the mass of adsorbent used (g).

The color removal efficiency (Y , %) was calculated from:

$$Y = \frac{C_0 - C}{C_0} \cdot 100 \quad (2)$$

where C_0 is the initial concentration of dye (mg·L⁻¹), and C is the concentration of dye after t minutes of adsorption (mg·L⁻¹).

The applicability of the kinetic and isotherm model to describe the adsorption process was validated by the normalized standard deviation, Δq (%), which is defined as [10]:

$$\Delta q(\%) = 100 \sqrt{\frac{\sum [(q_{\text{exp}} - q_{\text{cal}}) / q_{\text{exp}}]^2}{N - 1}} \quad (3)$$

where N is the number of data points, q_{exp} and q_{cal} ($\text{mg}\cdot\text{g}^{-1}$) are the experimental and calculated adsorption capacities, respectively. The lower the value of normalized standard deviation, the more accurate is the model that predicts the experimental data.

RESULTS AND DISCUSSION

Effect of GAC dose

Adsorbent dosage is one of the important parameter of adsorption. The effect of adsorption dosage was determined at a fixed initial dye concentration. The results illustrated in Figure 2 indicate that with the increase in adsorbent dose the percentage of adsorption increases.

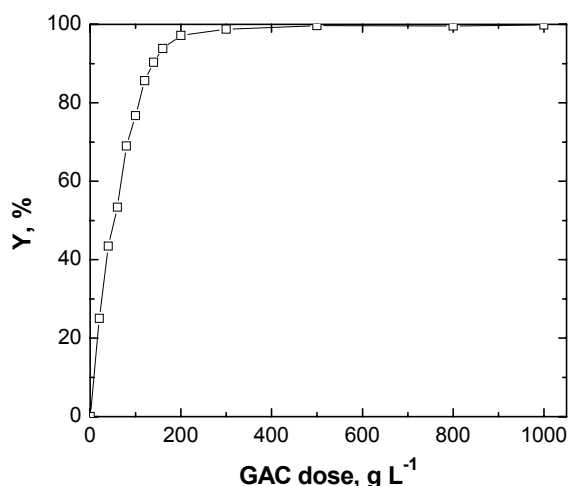


Figure 2. Effect of GAC dose on Indigo Carmine removal by adsorption ($C_0 = 20 \text{ mg}\cdot\text{L}^{-1}$)

In case of an initial concentration of dye of 20 ppm, a GAC dose of $0.2 \text{ g}\cdot\text{L}^{-1}$ resulted in a removal efficiency of 97.2%. A further increase in GAC dose did not lead to a significant improvement in removal efficiency.

Effect of solution pH

Selecting the appropriate pH of the effluent / wastewater for achieving maximum efficiency in the removal of dye by adsorption might be essential. Thus, the effect of pH on Indigo Carmine removal has been studied by varying the pH over a range of 3 to 11 and the obtained data are shown in Figure 3. It can be observed that the adsorption of Indigo Carmine onto the commercial GAC reached a maximum at the initial pH of 7.

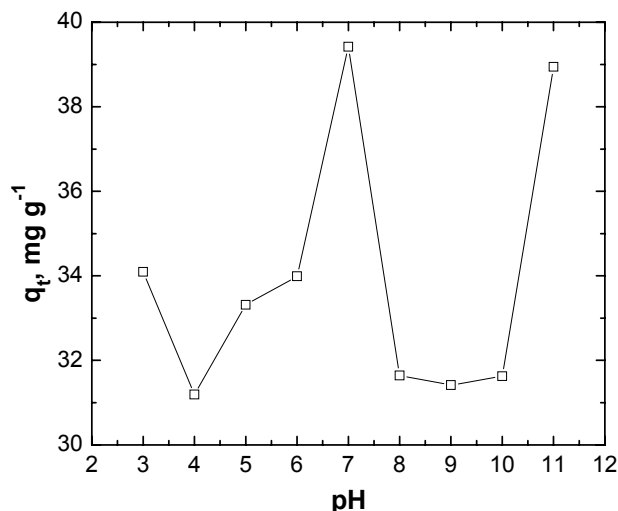


Figure 3. Effect of initial pH over the uptake of GAC

However, the pH value was not found to play an important role in the considered adsorption system, the effects due to textural properties of the adsorbent overwhelming those generated by chemical properties.

Effect of particle size

In Figure 4 is shown the effect of carbonaceous material particle size on the adsorption uptake. In this way, spherical grains of three different sizes (2, 3.5 and 7 mm in diameter) were used.

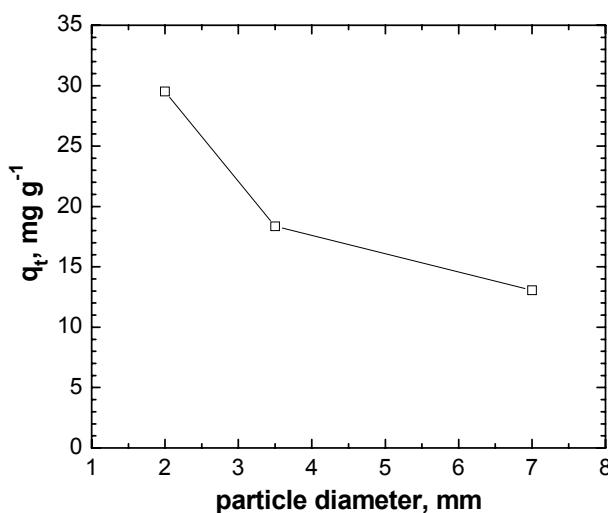


Figure 4. Effect of particle size over the uptake of GAC

As can be noticed, smaller particle size of GAC leads to higher values of dye uptake. This is explained by the higher specific surface of small-sized particle adsorbent.

Kinetics of Indigo Carmine adsorption on GAC

The solute uptake rate that controls the residence time of adsorbate uptake at the solid-solution interface was determined. Adsorption rate constants for the acid dye were calculated by using Lagergren [11], Ho [12], Elovich [13], Weber-Morris [14] and Bangham [15] models, which can be used to describe the mechanism of dye adsorption. The conformity between the experimental data and the model-predicted values was expressed by the correlation coefficients (R^2) and normalized standard deviation described by eq. (3).

Figure 5 presents the decolorization rate of Indigo Carmine adsorption on GAC at 295 K, $1 \text{ g}\cdot\text{L}^{-1}$ dose and 175 rpm at different initial concentrations of dye.

It can be noticed that the uptake increases with contact time until an almost constant value is reached, especially at lower concentrations of dye. At this point the amount of dye being adsorbed from the aqueous solution onto the activated carbon is in a state of dynamic equilibrium with the amount of dye desorbed.

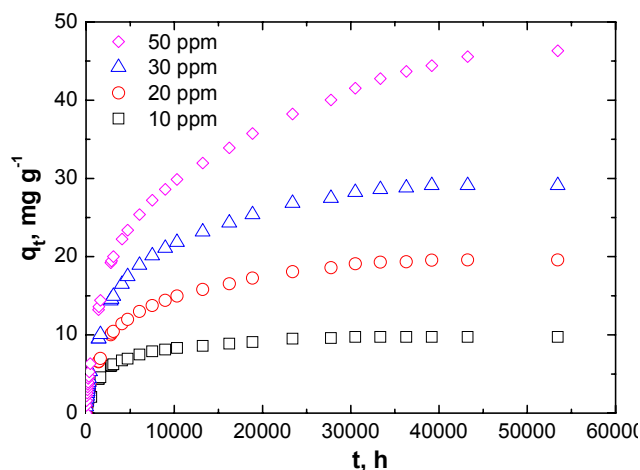


Figure 5. Kinetics of Indigo Carmine adsorption on GAC at different initial concentrations. Conditions: $1 \text{ g}\cdot\text{L}^{-1}$ GAC dose, 298.15 K, pH 5.5, 175 rpm

Lagergren has developed a conventional method used to describe the adsorption of an adsorbate from the liquid phase on a solid phase [11]. The linear form of pseudo-first-order equation is expressed by eq. (4). Figure 6a presents the Lagergren pseudo-first order kinetic plot for the adsorption of Indigo Carmine onto GAC, where the first order rate constant k_1 values and adsorption capacity q_e were calculated from the slope and the intercept (Table 1). Though R^2 values are relatively good, values of normalized standard deviation are also high which is due to the calculated q_e values are too low compared with experimental q_e values. Also, the estimated values of q_e predicted by this model are not close to the experimental values, which show that this model is not appropriate to describe the investigated adsorption process.

The pseudo-second-order equation is given by eq. (5). In the pseudo-second order model the rate of occupation of adsorption sites is proportional to the square of the number of unoccupied sites and the number of occupied sites is proportional to the fraction of the dye molecule adsorbed.

REMOVAL OF AN ACID DYE FROM AQUEOUS SOLUTION BY ADSORPTION ON A COMMERCIAL GRANULAR ACTIVATED CARBON: EQUILIBRIUM, KINETIC AND THERMODYNAMIC STUDY

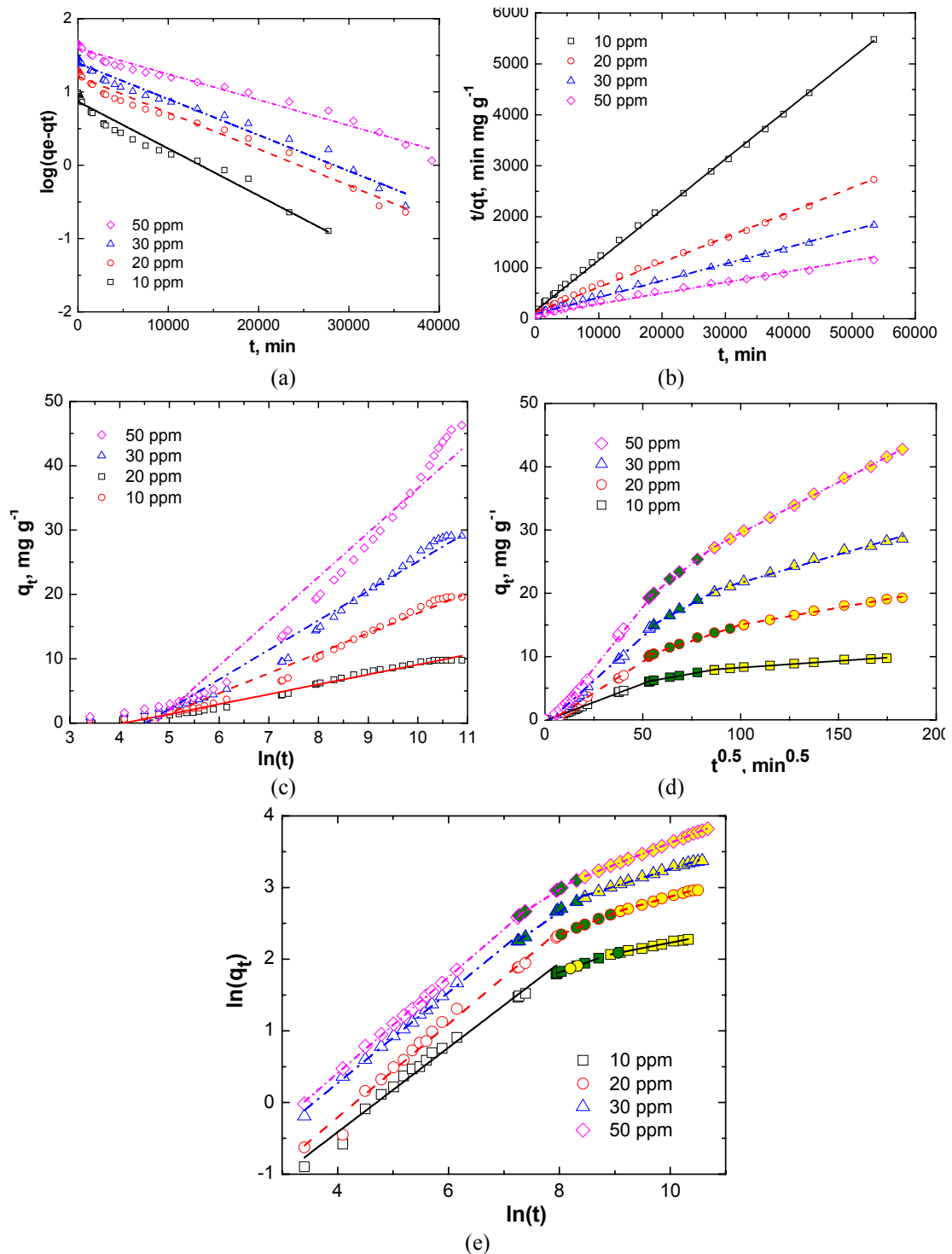


Figure 6. Lagergren (a), Ho (b), Elovich (c), Weber-Morris (d) and Bangham (e) models for (□) 10 mg/L, (○) 20 mg/L, (△) 30 mg/L and (◇) 50 mg/L of Indigo Carmine adsorption onto GAC

Table 1. Kinetic parameters of Lagergren, Ho, Elovich, Weber-Morris and Bangham models

| Model | Parameter | Initial concentration of dye, ppm | | | | Equation | Eq. no. | Ref. |
|----------------------------|---|-----------------------------------|---------|---------|---------|--|---------|------|
| | | 10 | 20 | 30 | 50 | | | |
| Lagergren | $q_{e,exp}, \text{mg}\cdot\text{g}^{-1}$ | 9.76 | 19.58 | 29.08 | | $\log(q_e - q_t) = \log q_e - \left(\frac{k_1}{2.303}\right) \cdot t$ | (4) | [11] |
| | $q_{e,cal}, \text{mg}\cdot\text{g}^{-1}$ | 7.39 | 16.34 | 24.64 | 39.27 | | | |
| | k_1, min^{-1} | 1.48E-4 | 1.14E-4 | 1.13E-4 | 8.08E-5 | | | |
| | R^2 | 0.967 | 0.982 | 0.981 | 0.978 | | | |
| | $\Delta q, \%$ | 67.08 | 57.24 | 57.86 | 59.91 | | | |
| Ho | $q_{e,cal}, \text{mg}\cdot\text{g}^{-1}$ | 10.00 | 20.45 | 30.39 | 47.17 | $\frac{t}{q_t} = \left(\frac{1}{k_2 \cdot q_e^2}\right) + \frac{1}{q_e} t$ | (5) | [12] |
| | $k_2, \text{g}\cdot\text{mg}^{-1}\cdot\text{min}^{-1}$ | 6.51E-5 | 1.89E-5 | 1.24E-5 | 5.76E-6 | | | |
| | R^2 | 0.999 | 0.997 | 0.996 | 0.989 | | | |
| | $\Delta q, \%$ | 16.84 | 18.98 | 22.44 | 24.09 | | | |
| Elovich | $\beta, \text{g}\cdot\text{mg}^{-1}$ | 0.63 | 0.32 | 0.22 | 0.145 | $q_t = \frac{1}{\beta} \ln(\alpha \cdot \beta) + \frac{1}{\beta} \ln(t)$ | (6) | [13] |
| | $\alpha, \text{mg}\cdot\text{g}^{-1}\cdot\text{min}^{-1}$ | 0.02 | 0.03 | 0.05 | 0.06 | | | |
| | R^2 | 0.980 | 0.971 | 0.965 | 0.955 | | | |
| | $\Delta q, \%$ | 26.17 | 26.24 | 26.89 | 27.59 | | | |
| Weber-Morris (first step) | $k_{id,1}, \text{mg}\cdot\text{g}^{-1}\cdot\text{min}^{-0.5}$ | 0.117 | 0.198 | 0.279 | 0.387 | $q_t = k_{id} \cdot t^{0.5} + c$ | (7) | [14] |
| | $c_1, \text{mg}\cdot\text{g}^{-1}$ | -0.130 | -0.696 | -0.800 | -1.532 | | | |
| | R^2 | 0.998 | 0.996 | 0.997 | 0.991 | | | |
| Weber-Morris (second step) | $k_{id,2}, \text{mg}\cdot\text{g}^{-1}\cdot\text{min}^{-0.5}$ | 0.056 | 0.102 | 0.168 | 0.238 | | | |
| | $c_2, \text{mg}\cdot\text{g}^{-1}$ | 3.127 | 4.802 | 5.755 | 6.773 | | | |
| | R^2 | 0.996 | 0.993 | 0.995 | 0.996 | | | |
| Weber-Morris (third step) | $k_{id,3}, \text{mg}\cdot\text{g}^{-1}\cdot\text{min}^{-0.5}$ | 0.021 | 0.054 | 0.089 | 0.154 | | | |
| | $c_3, \text{mg}\cdot\text{g}^{-1}$ | 6.147 | 9.643 | 12.829 | 14.217 | | | |
| | R^2 | 0.988 | 0.991 | 0.991 | 0.997 | | | |
| | $\Delta q, \%$ | 8.87 | 7.80 | 3.37 | 9.11 | | | |
| Bangham (first step) | $k_{r,1}, \text{mg}\cdot\text{g}^{-1}\cdot\text{min}^{-1}$ | 0.590 | 0.652 | 0.634 | 0.669 | $q_t = k_r \cdot t^{1/m}$ | (8) | [15] |
| | m_1 | -2.775 | -2.819 | -2.264 | -2.267 | | | |
| | R^2 | 0.985 | 0.988 | 0.996 | 0.999 | | | |
| Bangham (second step) | $k_{r,2}, \text{mg}\cdot\text{g}^{-1}\cdot\text{min}^{-1}$ | 0.279 | 0.304 | 0.534 | 0.488 | | | |
| | m_2 | -0.420 | -0.093 | -1.617 | -0.930 | | | |
| | R^2 | 0.998 | 0.998 | 0.985 | 0.995 | | | |
| Bangham (third step) | $k_{r,3}, \text{mg}\cdot\text{g}^{-1}\cdot\text{min}^{-1}$ | 0.151 | 0.217 | 0.240 | 0.314 | | | |
| | m_3 | 0.716 | 0.702 | 0.854 | 0.492 | | | |
| | R^2 | 0.995 | 0.994 | 0.993 | 0.999 | | | |
| | $\Delta q, \%$ | 6.70 | 7.16 | 2.33 | 1.98 | | | |

The q_e and k_2 values of the pseudo-second order kinetic model, eq. (3), can be determined from the slope and the intercept of the plots of t/q_t versus t . Figure 6b shows the linearized form of the pseudo-second order kinetic model. The correlation coefficients for the second order kinetic model were close to 1, and the predicted values of q_e agreed well with the experimental data. This suggests that the rate limiting step in this adsorption processes may be chemisorption involving valence forces through sharing or exchange of electrons between sorbent and sorbate [16].

The Elovich model is one of the most useful models for describing the kinetics of chemisorption of gas onto solid systems. However, recently it has been applied to describe the adsorption process of pollutants from aqueous solutions [17]. Chien and Clayton simplified the Elovich kinetics equation suggesting the eq. (6) [13]. The value of α is the adsorption quantity when $\ln(t)$ is equal to zero; i.e., the adsorption quantity when t is 1 h, while β gives an estimation of the number of sites available for adsorption [18].

The plots of q_t versus $\ln(t)$ of Elovich model for the adsorption of Indigo Carmine on GAC have been drawn in order to obtain the rate adsorption parameters as shown in Figure 6c.

The fitting to Elovich model seems to be not as good as the pseudo-second order kinetic model. Therefore, it can be stated that chemical binding reaction controls the sorption kinetic mechanism. So, the kinetics of Indigo Carmine adsorption using GAC as adsorbents can be better explained by the pseudo-second order model suggesting that adsorption rate was proportional to the number of unoccupied sites.

Taking into account that the kinetic results are fitted very well to a chemisorption model, the intraparticle diffusion model was plotted in order to verify the influence of mass transfer resistance on the binding of dye molecule to the GAC. When agitation speed is high enough, the thickness of the boundary layer surrounding the particle should be minimal and the boundary layer resistance or film diffusion should not be a major rate-controlling factor. Then, the intraparticle diffusion is the rate-limiting step and the uptake of the adsorbate varies with the square root of time. Thus, the plot of the square root of time versus the uptake (q_t) would result in a linear relationship, and the intraparticle diffusion would be the controlling step if this line passed through the origin.

When the plots do not pass through the origin, this is indicative of some degree of boundary layer control and this further show that the intraparticle diffusion is not the only rate controlling step, but also other processes may control the rate of adsorption. Such plots may present a multilinearity, indicating that two or more steps take place. The first, sharper portion is attributed to the diffusion of adsorbate through the solution to the external surface of adsorbent or the boundary layer diffusion of solute molecules. The second portion describes the gradual adsorption stage, where intraparticle diffusion is rate limiting. The third portion is attributed to the final equilibrium stage where intraparticle diffusion starts to slow down due to extremely low adsorbate concentrations in the solution [19].

Figure 6d shows the amount of dye adsorbed versus the square root of adsorption time for intraparticle transport of Indigo Carmine through the adsorbent materials. As noticed, the plots present a multilinearity, which indicated that three steps occurred in the process. The slopes of the linear portions indicate the rate of the adsorption process. Thus, the diffusion rates decrease with contact time due to the pores become smaller and smaller [20]. The first linear region is likely due to the adsorption into the mesopores of the adsorbent material, while the second linear section is most probable to represent the transition region from mesopores to micropores.

Kinetic data were further used in order to evaluate whether the pore diffusion is the only rate controlling step in the adsorption process by using Bagham's equation described in Table 1 [15]. The best agreement between experimental and predicted q_e values have been obtained with this Bangham's model. Thus, it can be stated the adsorption kinetics of Indigo Carmine adsorption on granular activated carbon is limited by pore diffusion. This conclusion is also supported by the microporous structure of GAC as emphasized by its textural characteristics determined by nitrogen adsorption isotherms.

However, in comparison with Ho's model, Bangham model presents three different stages and consequently three sets of parameters, while the pseudo second order kinetic parameters fits well the experimental data throughout the entire range of contact time.

Effect of Indigo Carmine initial concentration

As can be observed in Table 1, the increase of Indigo Carmine initial concentration results in an increase of the intraparticle rate parameters in the three portions, which is due to the augmentation of diffusion driving force that depends on the concentration gradient. The relationship between intraparticle rate parameters and initial concentration can be written as follows:

$$\ln(k_{id}) = \ln(A_i) + B_i \cdot \ln(C_0) \tag{9}$$

The effect of adsorbate concentration on the rate of intraparticle diffusion can be determined by plotting $\ln(k_{id})$ versus $\ln(C_0)$ as shown in Figure 7 and computing the values of correlations constants A and B as shown in Table 2.

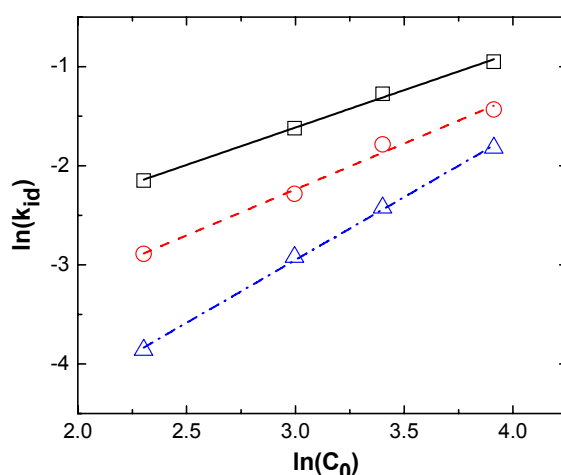


Figure 7. The $\ln(k_{id})$ versus $\ln(C_0)$ plots for (\square) the first, (O) second and (Δ) third linear segment of Weber model at Indigo Carmine adsorption on GAC

Table 2. Correlation values for the effect of concentration

| | A_i | B_i | R^2 |
|----------------------------|----------|-------|-------|
| First step ($k_{id,1}$) | 4.369E-4 | 0.754 | 0.997 |
| Second step ($k_{id,2}$) | 1.393E-4 | 0.926 | 0.992 |
| Third step ($k_{id,3}$) | 2.459E-5 | 1.268 | 0.999 |

The larger the effect of initial concentration on the intraparticle diffusion, the higher is the exponent of the slope (B value). Dye concentration has a much larger effect in the rate of intraparticle diffusion on GAC (larger value of B) in the third linear portion of Weber model. This is due to a larger influence of the driving force (higher dye concentration in solution) on the adsorption in micropores.

Equilibrium of Indigo Carmine adsorption on GAC

Adsorption isotherms pinpoint the distribution of adsorbed molecules between the liquid and solid phase when the equilibrium state is established. The equation parameters of isotherm models and their underlying thermodynamic assumptions might

provide important insights into the sorption mechanism and adsorbent properties. The obtaining of the best-fit isotherm has become more and more important as more applications are enhanced based on more accurate isotherms describing the adsorption systems. In order to optimize the use of adsorbents in removing dyes from effluent, it is essential to establish the most appropriate correlation. Thus, the modeling of equilibrium data is of great importance.

Therefore, an adsorption isotherm study was carried out on Langmuir [21] and Freundlich [22] isotherm models. The applicability of the isotherm models to the adsorption study done was compared based on the determination coefficients, R^2 , and normalized standard deviation values.

In Figure 8 are shown the equilibrium data obtained for the adsorption of Indigo Carmine on GAC at three different temperatures.

It can be noticed that the adsorption capacity of the GAC in relation to Indigo Carmine increases with temperature.

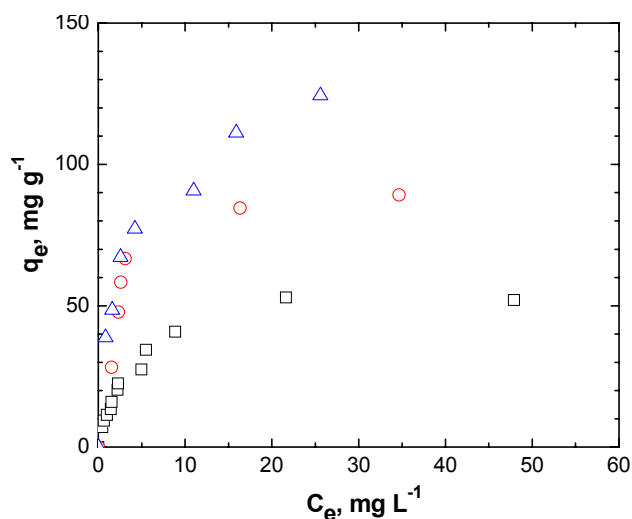


Figure 8. Equilibrium isotherms for IC-GAC system at 298 K (□), 308 K (○) and 318 K (△)

In Table 3 are listed the parameters of the isotherm models, while in Figure 9 are shown the linear-fit isotherms determined at three values of temperature.

The best values (close to unity) of the determination coefficient presented in Table 3 were obtained with Langmuir isotherm model, while the values of normalized standard deviation were rather lower than those obtained with Freundlich isotherm model, which underlines the adequacy of Langmuir model for this adsorption system.

The essential feature of the Langmuir isotherm can be expressed by means of dimensionless constant separation factor or equilibrium parameter, R_L , which is calculated using the following equation:

$$R_L = \frac{1}{1 + bC_0} \quad (12)$$

The calculated values of R_L are presented in Table 3. Since these values are ranged between 0 and 1, it can be stated that the process of Indigo Carmine adsorption on GAC is favorable.

Table 3. Parameters of investigated isotherms of Indigo Carmine adsorption onto GAC

| Isotherm model | Parameter | Temperature, K | | | Equation | Eq. no. | Ref. |
|----------------|---|----------------|-----------|-----------|---|---------|------|
| | | 298 | 308 | 318 | | | |
| Langmuir | $q_m, \text{mg} \cdot \text{g}^{-1}$ | 57.317 | 106.501 | 133.784 | $q_e = \frac{q_m \cdot K_L \cdot C_e}{1 + K_L \cdot C_e}$ | (10) | [21] |
| | $K_L, \text{L} \cdot \text{mg}^{-1}$ | 0.254 | 0.282 | 0.335 | | | |
| | R_L | 0.34-0.04 | 0.11-0.02 | 0.07-0.02 | | | |
| | R^2 | 0.996 | 0.993 | 0.986 | | | |
| | $\Delta q, \%$ | 9.378 | 15.227 | 12.602 | | | |
| Freundlich | $K_F, \text{mg} \cdot \text{g}^{-1} \cdot (\text{L} \cdot \text{mg}^{-1})^{-1/n}$ | 12.541 | 48.477 | 43.86 | $q_e = K_F \cdot C_e^{1/n}$ | (11) | [22] |
| | n | 2.172 | 5.75 | 3.021 | | | |
| | R^2 | 0.931 | 0.901 | 0.969 | | | |
| | $\Delta q, \%$ | 20.016 | 60.274 | 77.258 | | | |

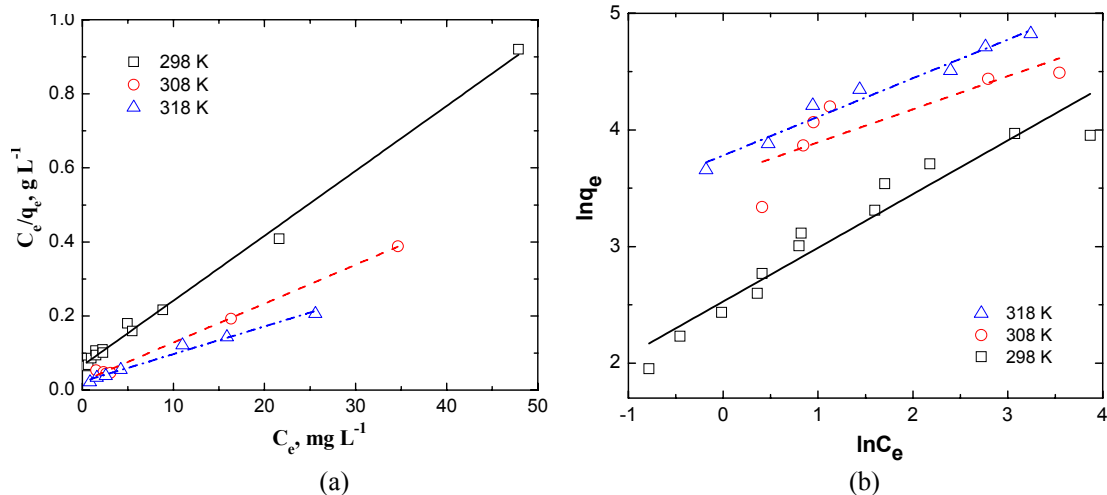


Figure 9. Adsorption isotherms Indigo Carmine adsorption onto GAC at several temperatures : (a) Langmuir, (b) Freundlich

Thermodynamics of Indigo Carmine adsorption on GAC

The adsorption capacity of the activated carbon increases with the increase in experimental temperature from 298 to 328 K [23]. The adsorption capacity depends on the thermodynamic parameters. The thermodynamic parameters of EBT sorption onto activated carbon were evaluated using the following equations [24]:

$$\Delta G = -R \cdot T \cdot \ln K_L \tag{13}$$

$$\ln K_L = -\frac{\Delta H}{R \cdot T} + const \tag{14}$$

$$\Delta G = \Delta H - T \cdot \Delta S \tag{15}$$

where ΔH , ΔS , ΔG and T are the enthalpy, entropy, Gibbs free energy and absolute temperature, respectively, R is the gas constant and K_L – the equilibrium constant.

According to data shown in Figure 10, the adsorption of Indigo Carmine onto GAC is an endothermic process which becomes more favorable with the increase of solution temperature.

Table 4. Thermodynamic parameters for Indigo Carmine adsorption onto GAC at different temperatures

| Temperature, K | ΔG , kJ/mol | ΔH , kJ/mol | ΔS , J/(mol·K) |
|----------------|---------------------|---------------------|------------------------|
| 298 | 3.40 | 10.894 | 25.06 |
| 308 | 3.241 | | |
| 318 | 2.893 | | |

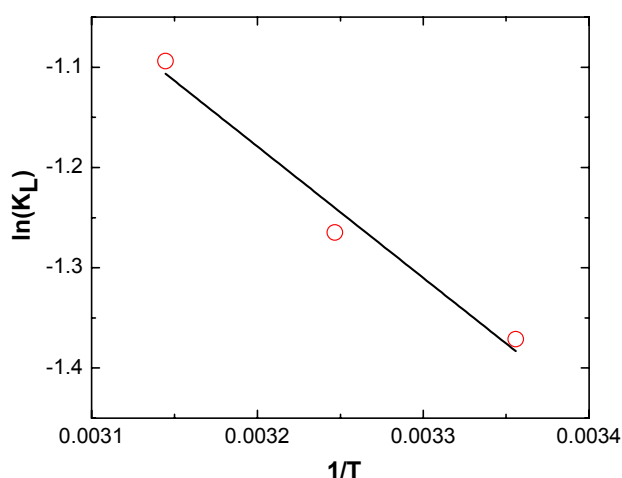


Figure 10. Dependence of $\ln(K_L)$ vs. $1/T$ for EBT adsorption onto GAC

However, the positive values of ΔG and ΔH indicate the presence of an energy barrier in the adsorption process [25]. The positive values of ΔH also show the endothermic nature of adsorption. The positive values of ΔS underline an increased disorder and randomness at the solid solution interface of the adsorbent [23].

CONCLUSIONS

In this work, an equilibrium and kinetic study of an acid dye adsorption on a commercial granular activated carbon was described. Indigo Carmine was used as model acid dye in order to evaluate the capacity of the considered GAC. It was found that Langmuir isotherm model best fit the equilibrium data. It was pinpointed that the adsorption capacity increases with temperature.

Lagargren, Elovich, Ho, Weber and Bangham models were employed in order to fit the kinetic data. Ho or pseudo-second order kinetic model was found to fit best the experimental kinetic data emphasizing the chemisorption of Indigo Carmine onto GAC. Also, the intraparticle diffusion mechanism of Indigo Carmine adsorption on the GAC was discussed. Based on Weber-Morris model, three steps were identified for the intraparticle diffusion process in the investigated adsorption system. As shown, the first one is due to the diffusion of dye into mesopores, the second one is due to the transition

region from mesopores to micropores, while the third step is due to the diffusion of dye in micropores.

The highest adsorption capacity ($133.8 \text{ mg}\cdot\text{g}^{-1}$) of GAC was obtained at $45 \text{ }^\circ\text{C}$.

According to the calculated thermodynamic parameters it was concluded that Indigo Carmine adsorption on GAC is an endothermic process.

NOMENCLATURE

c - a constant for any experiment (intraparticle diffusion model) ($\text{mg}\cdot\text{g}^{-1}$)

C - concentration of dye after t min. of adsorption ($\text{mg}\cdot\text{L}^{-1}$)

C_0 - initial Indigo Carmine concentration ($\text{mg}\cdot\text{L}^{-1}$)

C_e - concentration of dye solution at equilibrium ($\text{mg}\cdot\text{L}^{-1}$)

k_0 - constant (Bangham equation)

k_1 - the first-order reaction rate constant (min^{-1})

k_2 - the second-order reaction rate constant ($\text{g}\cdot\text{mg}^{-1}\cdot\text{min}^{-1}$)

k_{id} - intraparticle diffusion rate ($\text{mg}\cdot\text{g}^{-1}\cdot\text{min}^{-0.5}$)

K_F - constant of Freundlich isotherm ($\text{mg}\cdot\text{g}^{-1}\cdot(\text{L}\cdot\text{mg}^{-1})^{-1/n}$)

K_L - Langmuir isotherm constant ($\text{L}\cdot\text{mg}^{-1}$)

m - weight of adsorbent per liter of solution ($\text{g}\cdot\text{L}^{-1}$)

M_W - molecular weight ($\text{g}\cdot\text{mol}^{-1}$)

N - number of data points

q_{cal} - calculated adsorption capacity ($\text{mg}\cdot\text{g}^{-1}$)

q_e - amount of Indigo Carmine adsorbed at equilibrium ($\text{mg}\cdot\text{g}^{-1}$)

q_{exp} - experimental adsorption capacity ($\text{mg}\cdot\text{g}^{-1}$)

q_m - maximum monolayer coverage capacities ($\text{mg}\cdot\text{g}^{-1}$)

q_t - amount of dye adsorbed at time t ($\text{mg}\cdot\text{g}^{-1}$)

R - gas constant ($8.314 \text{ J}\cdot\text{mol}^{-1}\cdot\text{K}^{-1}$)

R_L - separation factor (dimensionless)

t - time (min)

T - temperature (K)

V - the solution volume (L)

W - mass of adsorbent used (g)

Y - color removal efficiency (%)

Greek letters

α - initial sorption rate ($\text{mg}\cdot\text{g}^{-1}\cdot\text{min}^{-1}$)

β - extent of surface coverage and activation energy for chemisorption ($\text{g}\cdot\text{mg}^{-1}$)

Δq - normalized standard deviation (%)

ACKNOWLEDGEMENTS

This work was supported by CNCSIS-UEFISCSU, project number PN II-RU No. 52/2010, COD 44.

REFERENCES

1. Alinsafi, A., da Motta, M., Le Bonte, S., Pons, M.N., Benhammou, A.: Effect of variability on the treatment of textile dyeing wastewater by activated sludge, *Dyes and Pigments*, **2006**, 69 (1-2), 31–39;
2. Oguz, E., Keskinler, B., Celik, Z.: Ozonation of aqueous Bomaplex Red CR-L dye in a semi-batch reactor, *Dyes and Pigments*, **2005**, 64 (2), 101–108;
3. Selcuk, H.: Decolorization and detoxification of textile wastewater by ozonation and coagulation processes, *Dyes and Pigments*, **2005**, 64 (3), 217–222;
4. Santhy, K., Selvaphaty, P.: Removal of reactive dyes from wastewater by adsorption on coir pith activated carbon, *Bioresource Technology*, **2006**, 97 (11), 1329–1336;
5. Can, O.T., Kobya, M., Demirbas, E., Bayranoglu, M.: Treatment of the textile wastewater by combined electrocoagulation, *Chemosphere*, **2006**, 62 (2), 181–187;
6. Secula, M.S., Cretescu, I., Petrescu, S.: An experimental study of Indigo Carmine removal from aqueous solutions by electrocoagulation, *Desalination*, **2011**, 277 (1-3), 277–235;
7. Chen, G. Lei, L., Hu, X., Lock, P.: Kinetic study into the wet air oxidation of printing and dyeing wastewater, *Separation and Purification Technology*, **2003**, 31 (11), 71–76;
8. Chiang, L.C., Chang, J.E., Tseng, S.C.: Electrochemical oxidation pretreatment of refractory organic pollutants, *Water Science and Technology*, **1997**, 36 (2-3), 123–130;
9. Xu, L., Zhao, H., Shi, S., Zhang, G., Ni, J.: Electrolytic treatment of C.I. Acid Orange 7 in aqueous solution using a three-dimensional electrode reactor, *Dyes and Pigments*, **2008**, 77 (1), 158–164;
10. Tan, I.A.W., Ahmad, A.L., Hameed, B.H.: Adsorption of basic dye on high-surface-area activated carbon prepared from coconut husk: Equilibrium, kinetic and thermodynamic studies, *Journal of Hazardous Materials*, **2008**, 154 (1-3) 337–346;
11. Langergren, S., Svenska, B.K.: Zur theorie der sogenannten adsorption geloster stoffe, *Veternskapsakad Handlingar*, **1898**, 24 (4), 1–39;
12. Ho, Y.S., McKay, G.: The kinetics of sorption of basic dyes from aqueous solution by sphagnum moss peat, *The Canadian Journal of Chemical Engineering*, **1998**, 76 (4), 822–826;
13. Chien, S.H., Clayton, W.R.: Application of Elovich equation to the kinetics of phosphate release and sorption in soils, *Soil Science Society of America Journal*, **1980**, 44 (2), 265–268;
14. Weber, W.J., Morris, J.C.: Kinetics of adsorption on carbon from solution, *Journal of the Sanitary Engineering Division*, **1963**, 89 (2), 31–59;
15. Aharoni, C., Sideman, S., Hoffer, E.: Adsorption of phosphate ions by collodion-coated alumina, *Journal of Chemical Technology and Biotechnology*, **1979**, 29 (7), 404–412;
16. Ho, Y.S., McKay, G.: Pseudo-second order model for sorption processes, *Process Biochemistry*, **1999**, 34 (5), 451–465;
17. Ozacar, M., Sengil, I.A.: A kinetic study of metal complex dye sorption onto pine sawdust, *Process Biochemistry*, **2005**, 40 (2) 565–572;
18. Tseng, R.L.: Mesopore control of high surface area NaOH-activated carbon, *Journal of Colloid and Interface Science*, **2006**, 303 (2) 494–502;
19. Crini, G., Peindy, H.N., Gimbert, F., Robert, C.: Removal of C.I. Basic Green 4 (Malachite Green) from aqueous solutions by adsorption using cyclodextrin-based adsorbent: Kinetic and equilibrium studies, *Separation and Purification Technology*, **2007**, 53 (1) 97–110;
20. Ip, A.W.M., Barford, J.P., McKay, G.: A comparative study on the kinetics and mechanisms of removal of Reactive Black 5 by adsorption onto activated carbons and bone char, *Chemical Engineering Journal*, **2010**, 157 (2-3), 434–442;
21. Langmuir, I.: The adsorption of gases on plane surfaces of glass, mica and platinum, *Journal of the American Chemical Society*, **1918**, 40 (9) 1361–1403;
22. Freundlich, H.: Concerning desorption in solutions, *Zeitschrift Fur Physikalische Chemie–Stoichiometrie Und Verwandtschaftslehre*, **1906**, 57 (4-6), 385–470;
23. Hema, M., Arivoli, S.: Comparative study on the adsorption kinetics and thermodynamics of dyes onto acid activated low cost carbon, *International Journal of Physical Sciences*, **2007**, 2 (1), 10–17;

24. Demirbas, A. Sari, A., Isldak, O.: Adsorption thermodynamics of stearic acid onto bentonite, *Journal of Hazardous Materials*, **2006**, 135 (1-3), 226–231;
25. Eren, E., Cubuk, O., Ciftci, H., Eren, B., Caglar, B.: Adsorption of basic dye from aqueous solutions by modified sepiolite: Equilibrium, kinetics and thermodynamics study, *Desalination*, **2010**, 252 (1-3), 88–96.